Virtual Screening for Novel Openers of Pancreatic K_{ATP} Channels

Emanuele Carosati,*,† Raimund Mannhold,*,‡ Philip Wahl,§ John Bondo Hansen,§ Tinna Fremming,§ Ismael Zamora,|| Giovanni Cianchetta,⊥ and Massimo Baroni▽

Laboratory for Chemometrics and Cheminformatics, Chemistry Department, University of Perugia, Via Elce di Sotto, 10, I-06123 Perugia, Italy, Department of Laser Medicine, Molecular Drug Research Group, Heinrich-Heine-Universität, Universitätsstrasse 1, D-40225 Düsseldorf, Germany, Diabetes Research Unit, Novo Nordisk A/S, Novo Nordisk Park, DK-2760 Maløv, Denmark, Lead Molecular Design, L., Valle's 96'102 (27) E-08190, Sant Cugat del Valle's, Spain, LexPharma, 350 Carter Road, Princeton, New Jersey 08540, and Molecular Discovery Ltd., 215 Marsh Road, HA5 5NE, Pinner, Middlesex, United Kingdom

Received December 18, 2006

Ligand-based virtual screening approaches were applied to search for new chemotype KCOs activating Kir6.2/SUR1 K_{ATP} channels. A total of 65 208 commercially available compounds, extracted from the ZINC archive, served as database for screening. In a first step, pharmacokinetic filtering via VolSurf reduced the initial database to 1913 compounds. Afterward, six molecules were selected as templates for similarity searches: similarity scores, obtained toward these templates, were calculated with the GRIND, FLAP, and TOPP approaches, which differently encode structural information into potential pharmacophores. In this way, we obtained 32 hit candidates, 16 via GRIND and eight each via FLAP and TOPP. For biological testing of the hit candidates, their effects on membrane potentials in HEK 293 cells expressing Kir6.2/SUR1 were studied. GRIND, FLAP, and TOPP all yielded hits, but no method top-ranked all the actives. Thus, parallel application of different approaches probably improves hit detection.

Introduction

Diabetes is becoming a global health problem, with an increasing number of people affected by either type 1 or type 2 forms. Whereas type 1 diabetes is characterized by rapid, autoimmune depletion of the insulin-producing pancreatic β-cells, type 2 diabetes is a slowly progressing disease affecting glucose and lipid homeostasis, frequently associated with obesity and elevated risk for cardiovascular diseases. Type 2 diabetes ultimately leads to β-cell degeneration, resulting in insufficient insulin release and the need for administration of exogenous insulin.

In pancreatic β-cells, ATP-sensitive potassium channels (K_{ATP} channels) couple changes in blood glucose concentrations to insulin secretion.[1] K_{ATP} channels also have important functions in various other tissues, and their structure and function have been described in detail.[2−7] K_{ATP} channels are octameric complexes of two protein subunits: the sulfonylurea receptor (SUR) and the pore-forming inwardly rectifying potassium channel (Kir). SUR proteins exist in the isoforms SUR1, SUR2A, and SUR2B; the pore-forming channels belong to the subfamily Kir6.0 exhibiting the isoforms Kir6.1 and Kir6.2. SUR1 combines with Kir6.2 to form the K_{ATP} channels of pancreatic β-cells, the cardiac and the skeletal muscle type consist of SUR2A and Kir6.2, and the smooth muscle type is composed of SUR2B and Kir6.1 or Kir6.2. K_{ATP} channel activity is regulated by cell metabolism, thereby linking the electrical activity of a cell to its metabolic state.

K_{ATP} channels represent promising drug targets.[8−10] Whereas certain sulfonylurea and benzoic acid insulin secretagogues are inhibitors (blockers), potassium channel openers (KCOs) stimulate potassium currents. KCOs comprise chemically extremely heterogeneous classes such as the cyanoguanidines (pinacidil, **1**), the benzopyrans (lev-cromakalim, **2**), and the 1,2,4-thiadiazines (diazoxide, **3**); for structures see Chart 1.

Whereas pinacidil and lev-cromakalim have little or no effect on K_{ATP} channels of β-cells,[11,12] diazoxide nonselectively activates both pancreatic and smooth muscle K_{ATP} channels.[13] Accordingly, the diazoxide molecule has been structurally modified to improve the selectivity profile. Variations of the size of the 3-alkyl substituent, in the substitution of position 7,[14,15] and in the introduction of 3-alkylamino side chains have been reported.[16,17] By combining components from the structures of pinacidil and diazoxide, Pirotte and co-workers[18,19] have prepared a series of pyrido[4,3-*e*]-1,2,4-thiadiazine 1,1-dioxides, among which BPDZ 44 (**4**), shown in Chart 1, was reported to be a more potent and selective KCO of pancreatic β-cells than diazoxide. These structures have subsequently been developed to include other potent benzo-1,2,4-thiadiazine 1,1-dioxide derivatives such as BPDZ 73 (**5**).[20] Replacing the pyridine or benzene moiety by thiophene resulted in a new series of thiophene-fused derivatives with improved potency and selectivity for Kir 6.2/SUR1 K_{ATP} channels.[21] Detailed structure−activity relationships of this series of compounds have been recently reviewed.[10] Prominent representatives of thienothiadiazine 1,1-dioxides are NNC 55-0118 (**6**) and NN414 (**7**); for structures see Chart 1.

Preclinical in vivo studies with **7** have demonstrated significant potential for the treatment of disorders resulting from excessive insulin release. Compound **7** reduced hyperinsulinemia in a dose-dependent manner in obese Zucker rats and improved glucose responsiveness.[22] Compound **7** has entered human clinical trials where it was found to inhibit insulin release 1 h postdosing in both healthy volunteers and type 2 diabetic patients. In the diabetic group, there was a trend toward improved β-cell secretory function.[23] Development of **7** was recently suspended, apparently because of elevated liver en-

* Corresponding authors: (E.C.) phone +39 075 5855550, fax +39 075 45646, e-mail emanuele@chemiome.chm.unipg.it; (R.M.) phone +49 211 8112759, fax +49 211 8111374, e-mail mannhold@uni-duesseldorf.de.
† University of Perugia.
‡ Heinrich-Heine-Universität.
§ Novo Nordisk A/S.
|| Lead Molecular Design.
⊥ LexPharma.
▽ Molecular Discovery Ltd.

10.1021/jm061440p CCC: $37.00
Published on Web 04/11/2007

Chart 1. [a]

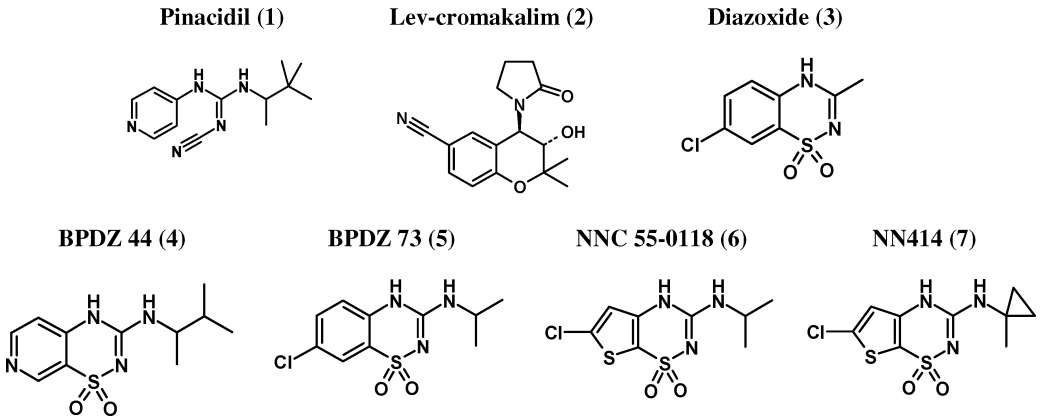

[a] First-generation KCOs lacking pancreas selectivity are shown in the first row; the second row gives structures of pancreas-selective KCOs comprising the chemical classes of pyridothiadiazine dioxides, benzothiadiazine dioxides, and thienothiadiazine dioxides.

zymes that were observed in the clinic. Accordingly, there is high interest in finding new chemical entities for drug development.

To search for new chemotypes, we applied ligand-based virtual screening (LBVS) approaches using different ways to encoding structural information into potential pharmacophores. The molecules found in this way were biologically tested for their effects on membrane potentials in HEK 293 cells expressing Kir6.2/SUR1.

Study Design

Virtual Screening. Exclusively ligand-based procedures[24,25] were applied. Whereas refined homology models of the K_{ATP} channel structure exist,[5−7] detailed knowledge on the 3D structure of complexes between KCOs and K_{ATP} channel binding sites is missing yet, which in turn excludes the application of structure-based virtual screening strategies.

A subset of roughly 65 000 commercially available compounds,[26] which covers a broad chemical landscape, was extracted from the ZINC database (release 5, January 2005),[27] as it is supplied via the World Wide Web.[28] One problem, when dealing with compound libraries of large size, is the treatment of, for example, chirality, protonation/deprotonation states, and tautomerism. Irwin and Shoichet[27] have already approached and solved this issue providing the ZINC database, which contains about 2.7 million substances that are distributed from different vendors. Each compound is provided in several different states; thus it can simultaneously approach the screening procedure with, for instance, diverse biologically relevant protonation states. At the end, when the database is refined, only the best ranked solution for each query molecule could be used for the final analysis: in all the statistics and numbers reported herein, each compound was therefore considered only once. The starting database consisted of 65 208 compounds, all of which are commercially available from the SPECS vendor.[26]

For database searching, several in silico methods were applied, reflecting both pharmacokinetic (PK) and pharmacodynamic (PD) aspects. First, the PK-related VolSurf procedure[29] was used to retain only compounds with druglike properties. In a second step, PD-related procedures were applied to rank the database molecules: GRIND[30] is based on molecular interaction fields (MIF), while the rather new methods FLAP and TOPP[31] are based on molecular fingerprints describing pharmacophore points.

Chemical Stability and Selection. Compounds that passed the PK filter, and that were top-ranked according to the PD-based similarity searches, were finally checked for chemical stability and toxicity by visual inspection. Removal of compounds with potential toxic and reactive functional groups followed basic medicinal chemistry criteria as well as literature suggestions.[32,33] In brief, the presence of the following chemical moieties served as criterion for removal: (a) five or more halogen atoms, (b) two or more cyano or nitro groups, (c) epoxide or aziride, (d) two or more aliphatic esters, (e) 1,2-dicarbonyl groups, (f) sulfonate and phosphonate esters, (g) aldehydes, (h) acyl or sulfonyl halides, (i) anhydrides, and (j) heteroatom−heteroatom single bonds, when not in a cycle or linked to aromatic/olefinic systems. These criteria were used to select the final sets of virtual hits out of the 200 compounds top-ranked by GRIND, FLAP, or TOPP, respectively. The overall procedure is summarized in Figure 1.

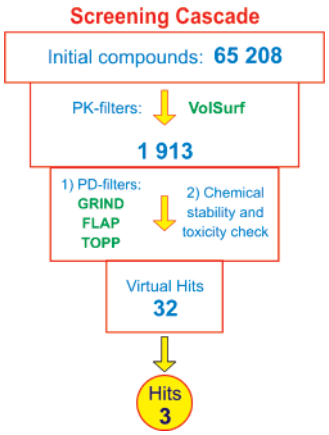

Figure 1. Schematized cascade for ligand-based virtual screening (LBVS). Pharmacokinetic filtering via VolSurf reduced the initial database of 65 208 structures to a set of 1913 compounds. For pharmacodynamic (PD) ranking, similarity scores were calculated with the GRIND, FLAP, and TOPP approaches versus six templates. In this way, we obtained 32 virtual hits. Biological testing in HEK 293 cells expressing Kir6.2/SUR1 yielded three actives.

Biological Testing of Virtual Hits. For screening the biological activities of the 32 virtual hits, their effects on membrane potentials in HEK 293 cells expressing Kir6.2/SUR1 were studied.[34−36]

Results and Discussion

Pharmacokinetic Filtering. The PK profile of the database compounds was determined by use of the VolSurf software;[37] for details see the Experimental Section. The 94 VolSurf

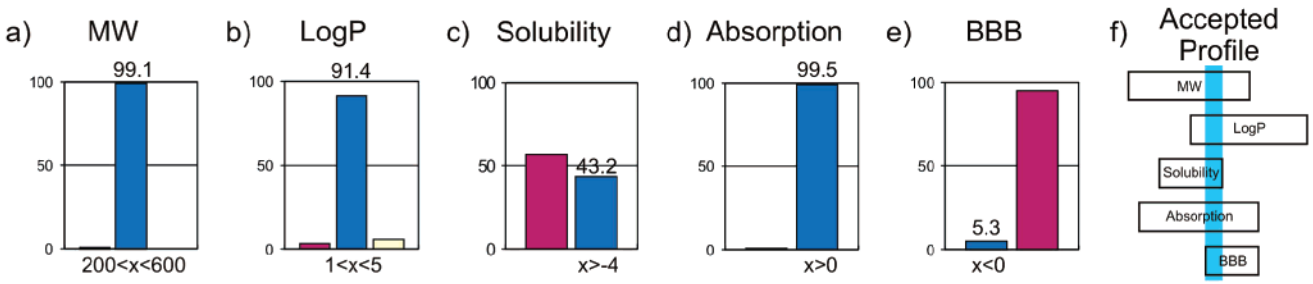

Figure 2. Results of PK filtering, separately schematized for (a) molecular weight, (b) log *P*, (c) solubility, (d) absorption, and (e) blood−brain barrier permeability (BBB). Blue bars represent the amount of the selected compounds. (f) Only a few compounds (cyan section) revealed good in silico PK profiles and passed all filters.

descriptors were obtained with a grid spacing of 0.5 Å and application of the GRID probes OH2, DRY, and O. The selection of compounds with a favorable PK profile was guided by the projection on predefined models available in the VolSurf model library.[38] A combination of PERL scripts provided this automated procedure for each data set molecule: (i) derivation of VolSurf descriptors, using the command-line version of the program; (ii) use of some common Volsurf descriptors, such as molecular weight (MW) and calculated log *P*, as well as prediction on pre-calculated VolSurf library models [blood−brain barrier (BBB), absorption, solubility][38] to derive the PK profile of the compound; and (iii) filtering according to the predefined PK settings described below.

In order to select compounds with sufficient solubility (at least 100 μM), the SOLY-min (minimum acceptable solubility) value was set to −4, where SOLY is expressed as log of the solubility, measured in moles per liter. The BBB-max (maximum acceptable permeability across the BBB) value was set to zero, in order to avoid data set compounds crossing the blood−brain barrier. The CACO2-min (minimum acceptable Caco2 passive permeability) value was set to zero, to guarantee adequate absorption. Standard drug size properties were selected via a molecular weight filter range between 200 and 600. Finally, an optimum lipophilicity profile was approached by a log *P* filter range between 1 and 5.

The results of pharmacokinetic filtering are schematically reported in Figure 2. Regarding molecular weight, log *P*, and absorption, the great majority of the data set compounds exhibit druglike properties. On the other hand, a drastic diminution of the virtual candidates occurs due to solubility and BBB filters. An acceptable solubility is predicted for only 43.2%, and the absence of BBB permeation for only 5.3%, of the initial data set compounds. Accordingly, the database size was significantly reduced from 65 208 to 1913, which equals an elimination of about 98%.

Pharmacodynamic Similarity Search. Three thienothiadiazine 1,1-dioxides (**8**−**10**)[21,34] and three benzothiadiazine 1,1-dioxides (**11**−**13**)[39] served as templates for ligand-based virtual screening. The synthesis of the six templates is described in the corresponding references, whereas the template structures are given in Chart 2 and their activity profiles in Table 1.

It is noteworthy that the thiadiazine substructures of all templates exhibit opposite H-bonding character: acceptor on the side of dioxide and donor on the side of NH moieties. In order to handle this peculiarity correctly, templates and data set molecules were described by means of 3D methods.

Similarity scores, obtained toward the templates, were calculated with different methods (see below). Each template was assigned a normalized weight, in order to reflect the relevance of the most actives (Table 1); the weight was tuned for modulating the relevance of templates on the scoring

Chart 2. Structures for the Six Molecular Templates[a]

	thienothiadiazine 1,1-dioxides	ref.		benzothiadiazine 1,1-dioxides	ref.
8	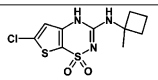	21	**11**	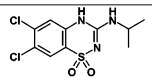	39
9	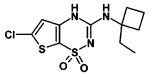	21	**12**	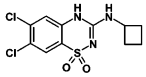	39
10	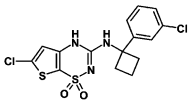	34	**13**	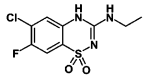	39

[a] Three thienothiadiazine 1,1-dioxides (**8**−**10**)[21,34] and three benzothiadiazine 1,1-dioxides (**11**−**13**)[39] served as templates for ligand-based virtual screening. Compounds **8** and **9** correspond to numbers **54** and **57** in the original paper. Compound **10** equals **1k** in ref 34, whereas compounds **11**, **12**, and **13** represent the derivatives **24**, **27**, and **32** in ref 39.

Table 1. Activity Profile for the Selected Templates

template	membrane potential βTC3[a] IC$_{50}$ (μM)	log 1/*C*	normalized weights[b] βTC3
8	0.014	7.85	1.00
9	0.1	7.00	0.71
10	0.16	6.80	0.64
11	0.28	6.55	0.58
12	1.25	5.90	0.36
13	0.20	6.70	0.63

[a] Repolarization of βTC3 cells. Data are from refs 21, 34, and 39. [b] Normalized weights (between 0.5 and 1.0) were assigned to the templates, reflecting the potency (βTC3; IC$_{50}$).

functions used in the PD filter. Compound 6-chloro-*N*-(1-methylcyclobutyl)-4*H*-thieno[3,2-*e*][1,2,4]thiadiazin-3-amine 1,1-dioxide (**8**) achieved the highest weight and 6-chloro-*N*-ethyl-7-fluoro-4*H*-1,2,4-benzothiadiazin-3-amine 1,1-dioxide (**13**) the lowest.

The 1913 remaining compounds were ranked according to the scores obtained from their similarity values toward the templates. For calculating the similarity values, the GRIND, FLAP, and TOPP approaches were used. Details are separately presented below.

PD-GRIND approach. Ten conformers were produced with CONFORT[40] for all 1913 compounds and in turn subjected to principal component analysis (PCA) using GRIND for description of the X-space. The GRIND descriptors were obtained from the default setting of the program Almond[41] and by applying the GRID probes DRY, O, and N1 in addition to the recently introduced shape probe TIP,[42] that describes the shape of the molecule via the same GRIND formalism.

A two-component model was selected to represent the chemical variation within the set, explaining about 40% of the variance (23.3% and 16.2% by the first and second principal

Table 2. Virtual Hits by the GRIND Approach[a]

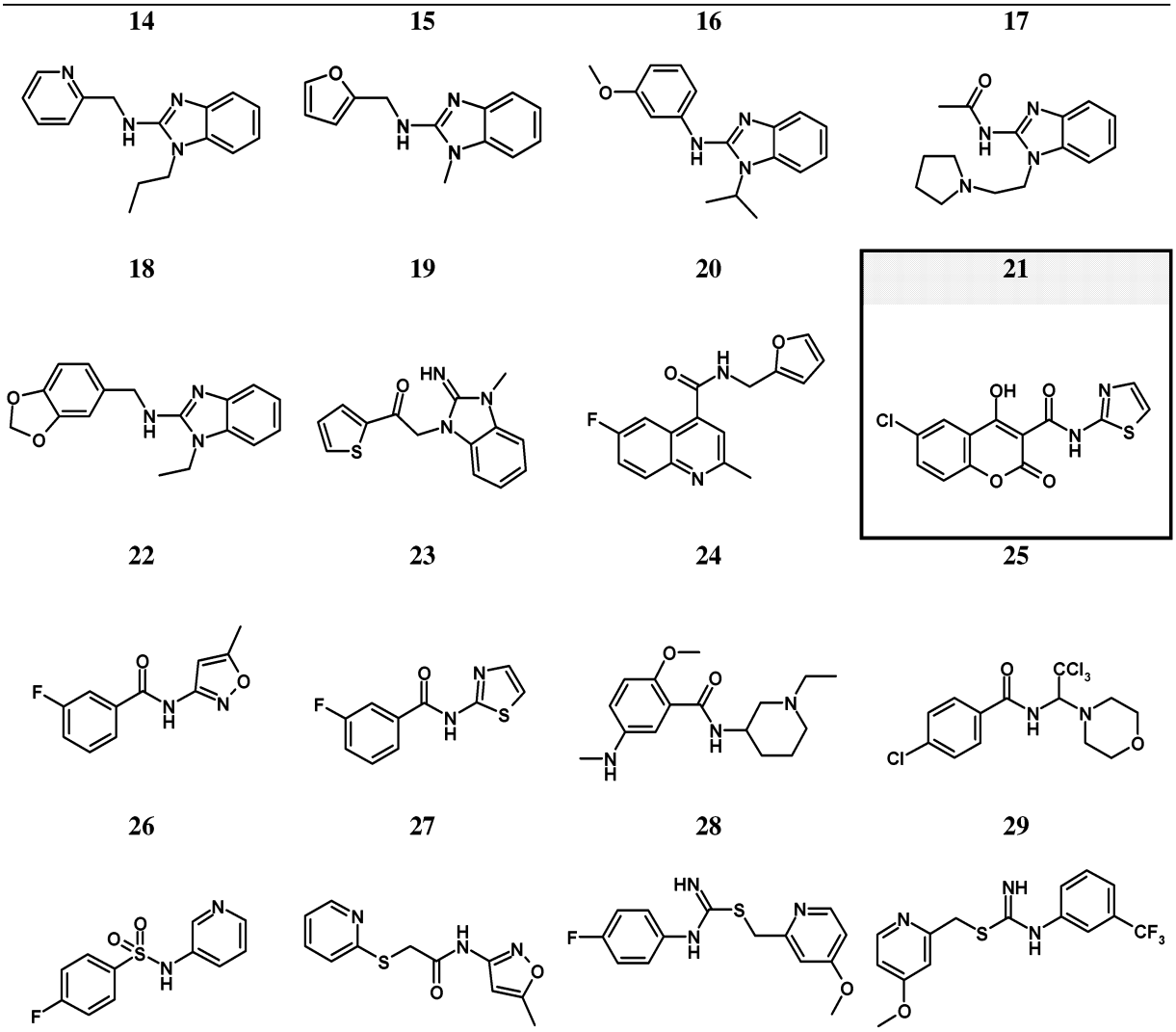

[a] Chemical structures of the 16 GRIND-derived virtual hits are shown. An imidazole moiety replaces in six cases the thiadiazine 1,1-dioxide moiety, present in the templates. Another common motif is the linkage of two preferably aromatic rings via amide, sulfonamide, or thiourea moieties. Compound **21** exhibited KCO potency in screening on pancreatic K_{ATP} channels.

component, respectively). The templates were then projected into the PCA model, and all pairwise distances (d_{it}) between object and template were derived from the 2D PC space. The normalized weights (w_t) for the six templates (t), listed in Table 1, multiplied by the object−template distances, were then summed in order to give the overall score. For molecule i it is defined as follows:

$$\text{GRIND score}_i = \sum_{t=1}^{6} w_t d_{it} \qquad (1)$$

The 200 compounds top-ranked on the basis of the GRIND approach were evaluated for chemical stability and potential toxicity according to the criteria described above. Among these 200 compounds, 16 were finally selected as virtual hits. Their structures are shown in Table 2. In six cases the thiadiazine 1,1-dioxide moiety, present in the templates, is replaced by an imidazole functionality. In eight cases, two preferably aromatic rings are bridged via linker moieties such as amide, sulfonamide, or thiourea.

PD-FLAP Approach. The novel FLAP (fingerprint for ligands and proteins) method[31] allows us to explore the 3D pharmacophoric space of ligands and proteins and to quantify their complementarity in the case of ligand−ligand, ligand−protein, or protein−protein comparisons.

From the six templates a supramolecular structure was built. With the program FLAP, all the molecules selected as templates were used to produce proposals of superposition, namely, supramolecular structures. Among all the proposals, the scoring values obtained are the guidelines to select the final multimolecular template (Figure 3), which was in turn used for fitting the database molecules.

The alignment procedure of test over template molecules is based on the superposition of potential 4-point pharmacophores (quadruplets). First, all template atoms are classified according to their chemical features as hydrophobic, hydrogen-bond (HB) donor, or HB acceptor. The GRID atom types are used to identify these pharmacophoric features. Then, a virtual fingerprint, called "pseudoreceptor", is defined via an exhaustive combination of all quadruplets formed by the template atoms.

The database compounds are described in the same way by encoding into potential 4-point pharmacophores; they are in turn searched for matching with the fingerprint of the template. Finally, the count of the common quadruplets defines the degree

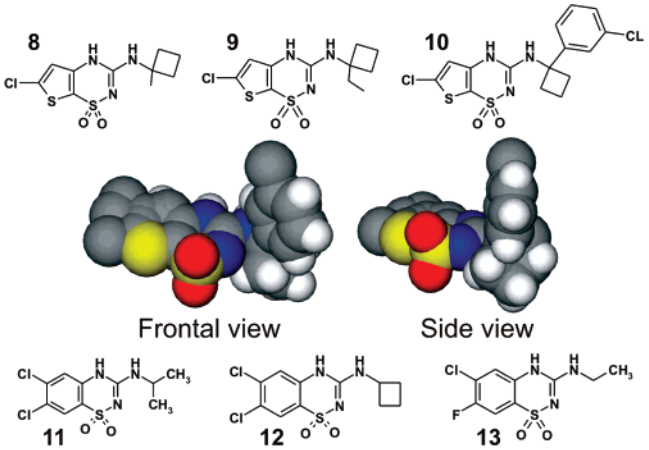

Figure 3. Multimolecular template generated from the superposition of six diverse compounds.

of pharmacophoric similarity between test molecule and template. A set of options tunes this procedure, which account for molecular shape and tolerance on assigning corresponding pharmacophoric features, as detailed in the Experimental Section. The number of common quadruplets (*ncq*) is then used as score for the test molecule *i*.

$$\text{FLAP score}_i = ncq_i \tag{2}$$

Out of the 200 compounds top-ranked via FLAP, eight remained as virtual hits after checking for chemical stability and potential toxicity; for structures see Table 3. FLAP-selected compounds exhibit a higher flexibility as compared with the template compounds. In six out of eight cases, the HB-accepting NH group, present in the templates, is replaced by a hydroxyl group.

PD-TOPP Approach. The TOPP method (triplets of pharmacophore points)[31] is based on a similar concept of pharmacophore derivation, described above for FLAP. Some differences, however, deserve mentioning: pharmacophoric triplets instead of quadruplets are considered, and the created fingerprint, which refers to the presence/absence of each triplet, can be stored for each data set molecule as well as for the templates. This allows multivariate analysis of the derived fingerprints, whereas only pairwise comparisons are carried out with the FLAP approach.

The 1913 retained compounds composed the set for the TOPP calculations that provided a large X-matrix of 2659 variables. The use of bitstrings for a very large set of different compounds biased the correlation between the variables: a principal component analysis of these data resulted in a three-component model, explaining only 31% of the variance. The six templates were then projected into the PCA model, and intermolecular distances were calculated between each test molecule *i* and each template *t*.

The same equation as for the GRIND approach was used: the already discussed normalized weights (w_t) for the six templates were multiplied by the object−template distances (d_{it}) derived from the 3D PC space. These products were then summed in order to give the overall score; it is defined for molecule *i* according to the following equation:

$$\text{TOPP} - \text{score}_i = \sum_{t=1}^{6} w_t d_{it} \tag{3}$$

By application of the identical steps, as outlined for the other approaches, finally eight compounds were selected as virtual hits from the 200 candidates top-ranked by TOPP. Their structures are given in Table 4. Six out of eight selected compounds have a rigid, bicyclic scaffold, closely mimicking the template structures. Carbonyl moieties as well as cyano substituents are frequently present.

Comparison of Methods. The simultaneous use of several methods for virtual screening is recommended in literature.[24,25] Diverse procedures give different rankings for the same group of compounds, and the performances of each method are often target-dependent and cannot be forecasted: the use of several and different approaches guarantees a more complete treatment of the data set.

In this case study, three different methods, GRIND, FLAP, and TOPP, were used for similarity search and three different rankings were obtained for the 1913 compounds. Interesting and experimentally confirmed hits were found with each of the three methods used. The relatively low number of actives, however, did not allow us to attribute superiority to one method over the others, because none of them was able to top-rank all three active compounds. Therefore, we focus in this section on compound selection rather than on the methods' capability to select biologically relevant hits.

Figure 4 is dedicated to compare the ranking of the selected compounds. By use of GRIND (see red line in Figure 4a), 16 molecules were selected among the first 200 top-ranked, as detailed above. The same compounds are randomly distributed within the data set, and the other two methods rank these selected as in random distribution. Among these two, TOPP (green) finds the GRIND selection with rankings that are a bit higher than random, whereas the FLAP (blue) ranking is below the random line. The eight FLAP-selected virtual hits (blue line in Figure 4b) are very low-ranked by the other two methods, with the two corresponding curves (red and green) below the random line. Finally, the eight TOPP-selected molecules (green line in Figure 4c) have been ranked by GRIND better if compared with the random distribution whereas definitively lower by FLAP, with only two among the first 1500 (i.e., about 75% of the data set).

Taken together, the three methods offer completely different selections of candidates: the minor resemblance between GRIND and TOPP is likely due to the approach via PCA, whereas the selection by means of FLAP is almost unique. Screening a database with multiple methods allows investigaton of different chemical landscapes and enhances the probability of finding chemically different hits.

In Vitro Screening of Virtual Hits. Glucose-induced insulin release is mainly a consequence of closure of K_{ATP} channels mediated by changes in the ATP/ADP ratio in the pancreatic β-cells. The closure leads to β-cell plasma membrane depolarization, influx of Ca^{2+} through voltage-gated calcium channels, increase in cytoplasmic Ca^{2+}, and activation of exocytosis of insulin from the pool of secretory granules. Compounds that open Kir6.2/SUR1 K_{ATP} channels will repolarize cell membranes of β-cells incubated in the presence of high glucose and will inhibit glucose-stimulated insulin release from β-cells and isolated islets.

To measure direct effects of the 32 virtual hits on K_{ATP} channels, a newly developed procedure was used to measure KCO-induced changes in membrane potential of HEK 293 cells expressing human Kir6.2/SUR1 channels.[35] The HEK 293 cell membranes were depolarized by the K_{ATP} channel blocker tolbutamide. Repolarization induced by the test compounds suggests that they either bind to the K_{ATP} channels to displace tolbutamide or increase ion currents by interaction with a site

Table 3. Virtual Hits by the FLAP Approach[a]

30	31	32	33
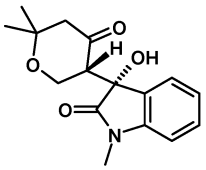	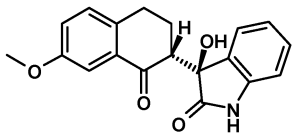	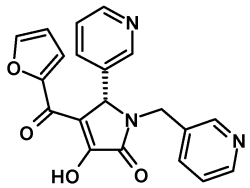	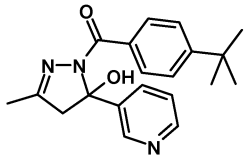
34	**35**	**36**	**37**
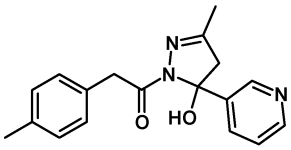	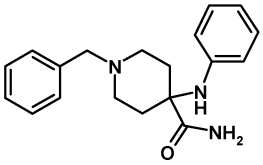	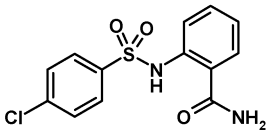	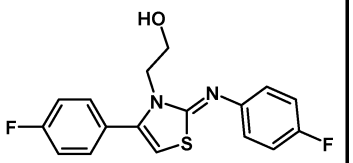

[a] Chemical structures of the eight FLAP-derived virtual hits are shown. These compounds exhibit much higher flexibility as compared to the templates. In six structures, the hydroxyl group replaces the NH group, present in the templates. Compound **37** exhibited KCO potency in screening on pancreatic K_{ATP} channels.

Table 4. Virtual Hits by the TOPP Approach[a]

38	39	40	41
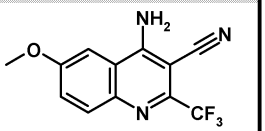	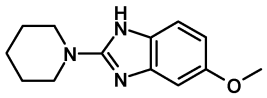	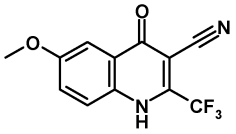	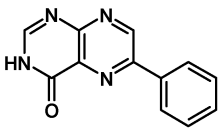
42	**43**	**44**	**45**
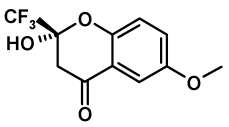	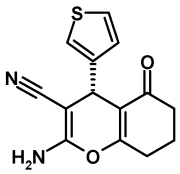	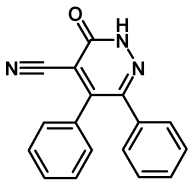	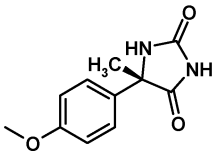

[a] Chemical structures of the eight TOPP-derived virtual hits are shown. Six compounds have a rigid, bicyclic scaffold and thereby closely resemble the template structures. Carbonyl moieties as well as cyano substituents are frequently present. Compound **38** exhibited KCO potency in screening on pancreatic K_{ATP} channels.

on the K_{ATP} channel different from the tolbutamide binding site. Previous studies have shown that the ability of structurally diverse KCOs to repolarize tolbutamide-induced membrane depolarization correlates with their ability to open K_{ATP} channels to inhibit insulin release (Table 5).[34,36]

EC_{50} values and E_{max} values are listed for comparison in Table 6. EC_{50} values represent the concentration needed to induce half-maximal change in fluorescence signal. E_{max} values, which reflect efficacy, were determined with 30 μM BPDZ 73 as reference. The compounds were normally tested only once. Exclusion criteria for further testing were EC_{50} values higher than 30 μM and E_{max} values lower than 40%. Active compounds were tested up to three times. As can be seen from Table 6, the majority of the virtual hits were inactive or weak openers of K_{ATP} channels.

Compounds *N*-[1-(2-pyrrolidin-1-ylethyl)-1*H*-benzimidazol-2-yl]acetamide (**17**), 6-chloro-4-hydroxy-2-oxo-*N*-1,3-thiazol-2-yl-2*H*-chromene-3-carboxamide (**21**), and 3-fluoro-*N*-1,3-thiazol-2-ylbenzamide (**23**), selected on the basis of the GRIND approach, caused a significant repolarization at the highest concentration tested (100 μM). The potency of the compounds was, however, too low for accurate estimates of EC_{50} values. The efficacies of **17** and **23** were below that of the reference BPDZ 73, whereas the efficacy of compound **21** was 1.5-fold higher. Among the FLAP-selected structures, compounds 2-{[(4-chlorophenyl)sulfonyl]amino}benzamide (**36**) and 2-[(2*Z*)-4-(4-fluorophenyl)-2-[(4-fluorophenyl)imino]-1,3-thiazol-3(2*H*)-yl]ethanol (**37**) were found to be active. The weak effect of compound **36** was observed at high concentrations (100 μM). Compound **37**, in contrast, caused a dose-dependent repolarization with an EC_{50} value of 21 $\pm$ 5.0 (n = 3) and an E_{max} value of 105.5% $\pm$ 4.9% (n = 3). Compounds 4-amino-6-methoxy-2-(trifluoromethyl)quinoline-3-carbonitrile (**38**), 5-methoxy-2-piperidin-1-yl-1*H*-benzimidazole (**39**), 6-phenylpteridin-4(3*H*)-one (**41**), and 3-oxo-5,6-diphenyl-2,3-dihydropyridazine-4-carbonitrile (**44**) caused a significant repolarization within the group of TOPP-selected structures. All four compounds were relatively weak KCOs with EC_{50} values above 15 μM. The

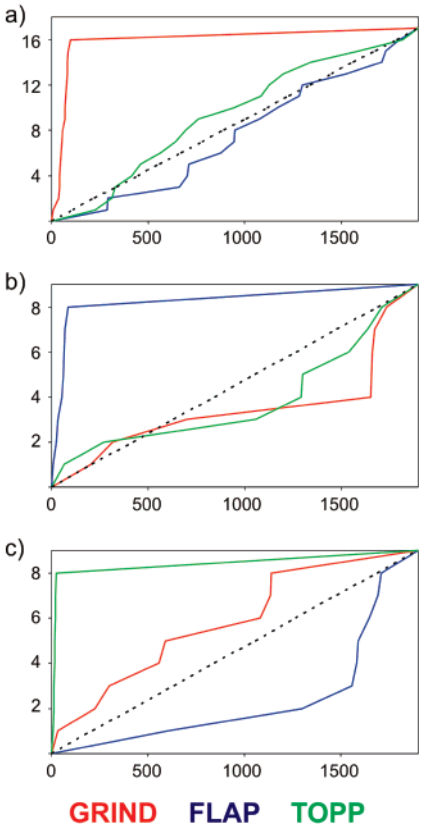

Figure 4. Enrichment curves for the compounds selected with the three methods. Each plot reports the ranking obtained by the three methods for the compounds selected by means of (a) GRIND, (b) FLAP, and (c) TOPP approach. The ranking line is red for GRIND, blue for FLAP, and green for TOPP, whereas the black dotted line, representing the random ranking, is reported for comparison.

Table 5. EC_{50} Values for NN414, BPDZ 73, and Diazoxide

compd	EC_{50} (μM) membrane potential[a]	activation of K^+ current[b]	membrane potential βTC3[c]	rat islets insulin release[d]
NN414 (**7**)	0.19 ± 0.06	0.45 ± 0.1	0.5 ± 0.1	0.21 ± 0.08
BPDZ 73 (**5**)	0.8 ± 0.01[e]	NT[f]	0.25 ± 0.02[e]	0.73 ± 0.05[g]
diazoxide (**3**)	33 ± 11	31 ± 5	13.7 ± 0.25	20.28 ± 8.82

[a] Repolarization of tolbutamide-depolarized HEK 293 cells expressing Kir6.2/SUR1 K_{ATP} channels. Shown are means ± SEM ($n \geq 3$). [b] Activation of whole-cell K^+ currents recorded from HEK293 cells stably expressing Kir6.2/SUR1. Shown are means ± SEM ($n \geq 3$). [c] Repolarization of glucose-depolarized β-TC3 cells. Shown are means ± SEM ($n \geq 3$). [d] Inhibition of insulin release from isolated rat islets, values are mean ± SEM of 4 experiments unless indicated; efficacy is above 77%. Data from ref 34. [e] Data from ref 36. [f] NT, not tested. [g] Data from ref 20.

effects of compounds **38**, **39**, and **41** were verified in 2−4 separate experiments. Compound **38** was found to be the most potent KCO of this series and dose-dependently induced repolarization with an EC_{50} of 15 ± 5.3 μM.

Taken together, screening on recombinant Kir6.2/SUR1 channels revealed compounds **21**, **37**, and **38** as the three hits out of 32 candidates. Dose−response curves for these hits are shown in Figure 5 in comparison with the reference compound BPDZ 73.

To further substantiate the observed activities, we determined the effects of compounds **21**, **37**, and **38** as well as the reference compound BPDZ 73 on glucose-stimulated insulin release from INS-1 cells. It has previously been shown that openers of Kir6.2/SUR1 K_{ATP} channels inhibits insulin release from β-cells and

Table 6. Biological Profile for the Selected Virtual Hits[a]

compd	SPECS name	EC_{50} (μM)	E_{max} (%)
BPDZ 73		0.25	100
	GRIND		
14	AE-848/42435319	NS	
15	AE-848/42435326	NS	
16	AF-399/42487749	NS	
17	AE-848/36047047	>30	55
18	AE-848/11420668	NS	
19	AE-848/36049010	NS	
20	AF-399/42385149	NS	
21	AE-406/41056766	>30	171; 147
22	AA-504/07988017	NS	
23	AA-504/08310047	>30	35; 88
24	AE-641/30152040	NS	
25	AF-399/32478006	NS	
26	AG-205/09314063	NS	
27	AA-768/33245042	NS	
28	AE-641/01085024	NS	
29	AE-641/01085027	NS	
	FLAP		
30	AE-848/34161052	NS	
31	AG-205/37159123	NS	
32	AF-399/41319387	NS	
33	AG-205/37159126	NS	
34	AG-205/37159041	NS	
35	AE-641/03239053	NA	
36	AG-670/36669035	>30	47
37	AG-205/37106157	21 ± 5.0	105 ± 4.9
	TOPP		
38	AG-687/25019010	15 ± 5.3	160 ± 54
39	AE-848/36959511	22; >30; >30	52 ± 6.3
40	AG-687/25019011	NS	
41	AC-907/34132003	>30; 13	55; 84
42	AF-407/36112021	NS	
43	AG-205/11317012	NS	
44	AE-406/41057003	>30	55
45	AG-690/34444027	NS	

[a] For the 32 virtual hits, EC_{50} (micromolar) and E_{max} (percent) values are given for KCO-induced changes in membrane potential of HEK 293 cells expressing human Kir6.2/SUR1 channels. The HEK 293 cell membranes were depolarized by the K_{ATP} channel blocker tolbutamide. NA, not active; NS, not significant.

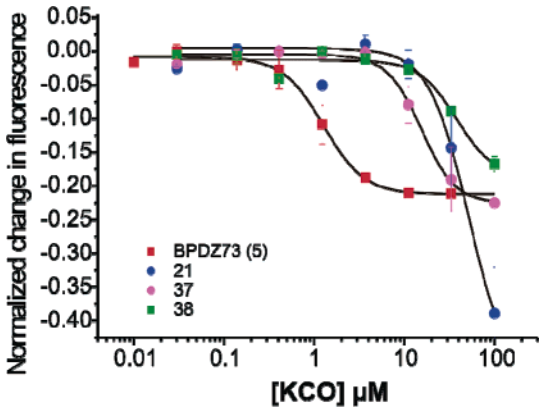

Figure 5. Dose−response curves for the three hits **21**, **37**, and **38**, in comparison with the reference compound BPDZ 73. The assay measures KCO-induced changes in membrane potential on HEK293 cells with recombinant expression of human Kir6.2/SUR1 by use of a fluorescent membrane potential kit and a conventional 96-well fluorescence plate reader. Each data point represents the mean fluorescence value from three separate wells and the experiment was repeated three times with similar results.

islets and that there is a correlation between the ability to hyperpolarize β-cell membranes and to inhibit insulin release; for further details see ref 21 and Table 5. As shown in Figure 6, compounds **21**, **37**, **38**, and BPDZ 73 efficiently inhibit insulin

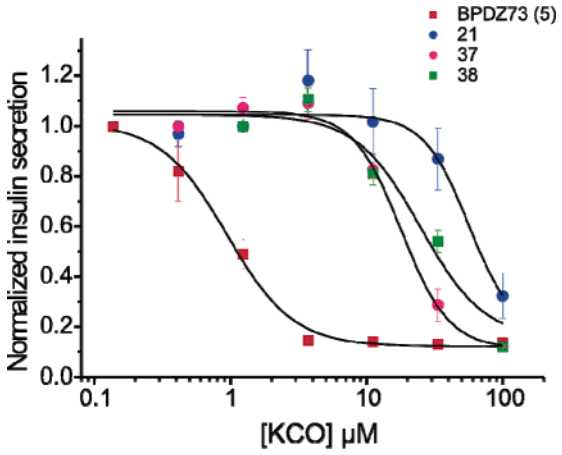

Figure 6. KCO-induced inhibition of glucose-stimulated insulin release from INS-1 cells for the three hits **21**, **37**, and **38**, in comparison with the reference BPDZ 73. INS-1 cells were incubated with test compounds at different concentrations at 15 mM glucose. Each data point represents the mean of 3−4 experiments.

release with IC_{50} values of 56 ± 11 μM, 18 ± 2.7 μM, 25 ± 7.5 μM, and 0.94 ± 0.12 μM, respectively. The potencies are in close agreement to those observed in the membrane potential assay, supporting that these compounds are openers of K_{ATP} channels of the β-cells.

Conclusion

In pharmaceutical research, virtual screening has become a widely used approach and an integral part of many drug discovery efforts. We applied such techniques in a search for novel openers of pancreatic K_{ATP} channels. In this pharmacological class, there is particular interest in finding new chemical entities due to lacking selectivity of currently available compounds as well as recent suspension of clinical candidates. We used exclusively ligand-based procedures, because 3D structures of complexes between KCOs and K_{ATP} channel binding sites are missing yet.

Typically, virtual screening approaches involve database filtering to exclude compounds containing toxic, reactive, or otherwise undesired groups. VolSurf was used for such filtering in a database of 65 000 compounds. Among the filter functions applied, low solubility and/or high brain permeability were mainly responsible for a strong data set reduction.

In the second step, ligand-based virtual screening approaches focus on comparative molecular similarity analysis of compounds with known and unknown activity. For calculating the similarity values, the programs GRIND, FLAP, and TOPP were used. They differently encode structural information into potential pharmacophores. GRIND[43] and FLAP[44] were already used successfully for LBVS. Finally, 32 virtual hits were achieved via similarity analysis.

Biological testing resulted in three hits. GRIND, FLAP, and TOPP yielded one hit each, which significantly differ from each other and from the starting templates. None of the three methods used was able to top-rank all actives; these findings confirm that the parallel application of different approaches enhances the probability of hit detection. These new chemotypes can be used as starting point to find novel openers of pancreatic K_{ATP} channels; systematic variations around the hit structures are currently under investigation.

Experimental Section

A. Databases. The SPECS data set used for screening is part of release 5 of the ZINC archive,[27] downloaded on January 2005 from the ZINC web site http://zinc.docking.org.

B. Biological Assays: 1. Cell Culture. HEK 293 stably expressing human SUR1 and Kir6.2 were cultured at 37 °C in a humidified atmosphere of 95% air and 5% CO_2 in Dulbecco's modified Eagle's medium with 4.5 g/L glucose supplemented with 10% fetal calf serum (FCS), penicillin (100 units/mL), and streptomycin (0.1 mg/mL) plus 44 μg/mL hygromycin and 0.6 mg/mL G418 as selection medium.[45] Cells are seeded out in poly-(lysine)-coated microtiter plates at 50 000 cells/well and cultured for 2 days in 100 μL/well culture medium before the day of the experiment.

Rat insulinoma-derived INS-1E cells, derived from parental INS-1 cells, were obtained from Claes B. Wollheim, University Medical Center, Geneva, Switzerland.[46] INS-1E cells were cultured in a humidified atmosphere containing 5% CO_2 in RPMI 1640 medium (Gibco 61870-010) supplemented with 50 μM 2-mercaptoethanol, 10% fetal bovine serum, 100 units/mL penicillin, and 100 μg/mL streptomycin. The maintenance culture was passaged once a week by gentle trypsinization and seeded in Nunc culture flasks. For all insulin release experiments, INS-1E cells were seeded at 50 000 cells/well in Nunc 96-well plates and used 2−3 days thereafter.

2. Membrane Potential Studies in HEK 293 Cells Expressing Kir6.2/SUR1. K_{ATP} channel activity was monitored by evaluating changes in membrane potential, by use of a membrane potential kit (Molecular Devices). Assays were carried out in black clear-bottomed 96-well plates at 34 °C on a NovoStar machine (BMG, Germany) and K_{ATP} channels were activated by the addition of the K_{ATP} channel opener in a mixed assay medium [loading buffer and Hanks' balanced salt solution (HBSS, Molecular Devices and Gibco)] plus 10 μM tolbutamide to suppress constitutive K_{ATP} channel activity. Changes in fluorescence were measured with an excitation wavelength of 490 nm and an emission wavelength of 550 nm, before and 5−10 min after addition of test compounds. Measurement data were exported over to MS Excel where a before/after subtraction and normalization to the measurement level preceding any addition was made. Concentrations of test and control (BPDZ 73, 7-chloro-3-isopropylamino-4*H*-1,2,4-benzothiadiazine 1,1-dioxide)[21] compounds were compared and E_{max} values were determined with BPDZ 73 as the reference at 30 μM. Data from three parallel runs on the same plate were copied to Graph Pad Prism where a four-parameter logistic curve fit was made (Hill slope locked at −1.5) for each run of eight points separately.

3. Insulin Secretion Studies in INS-1E Cells. Before the secretory responses to test compounds and glucose were tested, cells were maintained for 30 min in glucose-free Krebs Ringer bicarbonate HEPES (KRBH) buffer: 115 mM NaCl, 4.7 mM KCl, 5 mM $NaHCO_3$, 1.2 mM KH_2PO_4, 1.2 mM $MgSO_4$, 2.6 mM $CaCl_2$, 2 mM L-glutamine, and 20 mM *N*-(2-hydroxyethyl)piperazine-*N*′-ethanesulfonic acid (HEPES), pH 7.4, with bovine serum albumin (BSA, 0.2%) (Sigma A-7888). The glucose-free KRBH was aspirated and cells were further incubated for 120 min in KRBH with test compounds and 15 mM glucose. The incubation was stopped by transferring the supernatant to a new 96-cell plate (Greiner minisorp) through a filter plate (Millipore MADV N6510). The supernatant was store at −20 °C, and insulin was measured by radioimmunoassay (RIA) with rat insulin as standard.

4. Data Analysis. The results were analyzed in Prism (GraphPad Software) with a four-parameter logistic equation to extract IC_{50} and E_{max} values. SEM was calculated for all compounds.

C. VolSurf. VolSurf is a program to transform 3D energy maps into molecular descriptors. In the VolSurf procedure, first the GRID[47,48] force field is applied to characterize potential polar and hydrophobic interaction sites around target molecules by the water (OH2), the hydrophobic (DRY), and the hydrogen-bonding acceptor carbonyl oxygen (O) probe. Afterward, molecular descriptors are calculated from these 3D maps. They refer to molecular size and

shape, to hydrophilic and hydrophobic regions and to the balance between them. Chemometric tools can be used to relate the VolSurf descriptor matrix with ADME properties: in the library models, projection in latent variables are used quantitatively (PLS) to correlate with aqueous solubility or qualitatively (PLS-DA) to classify compounds according to high or low intestinal absorption or brain membrane permeability. The used version 4.1 comprises 94 descriptors covering biologically relevant properties such as shape, surface and volume, electrostatic forces, hydrogen bonding, and lipophilicity.

D. GRIND. Grid-independent descriptors (GRIND)[30] were generated by the software Almond, version 3.3.[41] GRIND have been designed mainly to represent pharmacodynamic properties, starting from molecular interaction fields computed on the basis of the GRID force field.[47,48] When molecular interaction fields (MIF) are computed for a data set molecule, the nodes showing favorable energies of probe−molecule interaction represent positions where groups of a receptor, mimed by the probe, would interact favorably with the molecule. Hence, by use of different probes, one obtains a set of such positions that define a virtual receptor site. The procedure involves three steps: (i) computing a set of MIF, (ii) filtering the MIF to extract the most relevant regions, and (iii) encoding the filtered MIF into the GRIND variables. These variables refer to the field energy of node pairs and to the corresponding distance, and they represent the pharmacophoric regions of a virtual receptor and their interactions with the molecular candidate. The shape descriptors are also represented in a correlogram-like form, where the autocorrelograms describe the distance between certain regions defining the spatial extent of the molecule and the cross-correlograms describe the distance between these regions and other pharmacophoric regions described above.

E. FLAP. The procedure FLAP[31] (fingerprint for ligands and proteins) was recently developed for a fingerprint-type description of both ligands and protein binding sites. FLAP classifies all the heavy atoms of ligand molecules as hydrophobic, hydrogen-bond donating or accepting, and positively or negatively charged, but other properties can also be specified in more detail. It describes each molecule as a set of quadruplets, derived by combining all the atoms, four by four, in an exhaustive way. Each quadruplet is defined by the character of its composing atoms, by their six interatomic distances, measured in angstroms and binned in 1 Å intervals, and by an additional flag for the chirality of the quadruplet. The huge amount of information obtained is then documented in a fingerprint mode where the absence or presence of all tetrahedrals corresponds to 0 or 1, respectively. For computational reasons, only presences are stored in such a way that facilitates further searches and uses. The options (flags) used for the FLAP calculations are briefly summarized: (1) the tolerance between pairwise atoms (from template and data set molecule) was set to 1 Å ($b = 1$); (2) only 20% of test-molecule atoms were allowed to lie out of the template molecular volume ($c = 0.4$); (3) the pseudocavity defined by the molecular template was dilated by 2 Å of thickness ($d = 2$); (4) up to 10 rotatable bonds were considered and automatically selected within each molecular structure ($r = 10$); and (5) up to 50 conformers were generated for each data set molecule, and the best results obtained among these was the result assigned to the compound ($s = 50$).

F. TOPP. The recently developed TOPP procedure[31] classifies each atom as either hydrophobic (DRY), or hydrogen-bonding acceptor (HBA) or donor (HBD), according to the GRID classification,[47] which takes into account geometry, hybridization, and neighboring. In case of hydrogen-bonding capabilities as both acceptor and donor, the atom is considered twice, once as acceptor and once as donor. Distances are computed between all the atoms from the molecule with a tolerance of 1.5 Å, that is, the same order of many covalent bonds. The entire set of combinations of three different atoms is produced and encoded into a unique vectorial description, which is composed of thousands of variables (in this case about 22 000) and can be handled with statistics and chemometrics tools, such as GOLPE software.[49,50] The amount of variables is strongly reduced to a lower value because many of them are simply null but exist because a fixed structure of the data; in this case, only 2659 were active variables. The options (flags) used for the TOPP calculations are briefly summarized: (1) the presence/absence option (flag b) was used; (2) HB donor/acceptor atoms were split into donors and acceptors (flag s); (3) the distance between bins was set to 1.5 Å ($d = 1.5$); and (4) a maximum of 50 conformations were generated on-the-fly ($s = 50$) by use of up to 10 rotatable bonds ($c = 10$): thereby, the final molecular fingerprint took into account the triplets from all the conformations generated.

References

(1) Ashcroft, F. M.; Rorsman, P. ATP-Sensitive K^+ Channels: a Link between B-Cell Metabolism and Insulin Secretion. *Biochem. Soc. Trans.* **1990**, *18*, 109−111.

(2) Aguilar-Bryan, L.; Bryan, J. Molecular Biology of Adenosine Triphosphate-Sensitive Potassium Channels. *Endocr. Rev.* **1999**, *20*, 101−135.

(3) Seino, S. ATP-Sensitive Potassium Channels: a Model of Heteromultimeric Potassium Channel/Receptor Assemblies. *Annu. Rev. Physiol.* **1999**, *61*, 337−362.

(4) Ashcroft, F. M.; Gribble, F. M. ATP-Sensitive K^+ Channels and Insulin Secretion: Their Role in Health and Disease. *Diabetologia* **1999**, *42*, 903−919.

(5) Ashcroft, F. M. ATP-sensitive potassium channelopathies: focus on insulin secretion. *J. Clin. Invest.* **2005**, *115*, 2047−2058.

(6) Bryan, J.; Crane, A.; Vila-Carriles, W. H.; Babenko, A. P.; Aguilar-Bryan, L. Insulin Secretagogues, Sulfonylurea Receptors and K_{ATP} Channels. *Curr. Pharm. Des.* **2005**, *11*, 2699−2716.

(7) Moreau, Chapter; Prost, A.-L.; Dérand, R.; Vivaudou, M. SUR, ABC Proteins Targeted by K_{ATP} Channel Openers. *J. Mol. Cell. Cardiol.* **2005**, *38*, 951−963.

(8) Coghlan, M. J.; Carroll, W. A.; Gopalakrishnan, M. Recent Developments in the Biology and Medicinal Chemistry of Potassium Channel Modulators: Update from a Decade of Progress. *J. Med. Chem.* **2001**, *44*, 1627−1653.

(9) Mannhold, R. K_{ATP} Channel Openers: Structure−Activity Relationships and Therapeutic Potential. *Med. Res. Rev.* **2004**, *24*, 213−266.

(10) Hansen, J. B.; Arkhammar, P. O. G.; Bodvarsdottir, T. B.; Wahl, P. Inhibition of Insulin Secretion as a New Drug Target in the Treatment of Metabolic Disorders. *Curr. Med. Chem.* **2004**, *11*, 1595−1615.

(11) Moreau, Ch.; Jacquet, H.; Prost, A. L.; D'hahan, N.; Vivaudou, M. The Molecular Basis of the Specificity of Action of K_{ATP} Channel Openers. *EMBO J.* **2000**, *19*, 6644−6651.

(12) Reimann, F.; Gribble, F. M.; Ashcroft, F. M. Differential Response of K_{ATP} Channels Containing SUR2A or SUR2B Subunits to Nucleotides and Pinacidil. *Mol. Pharmacol.* **2000**, *58*, 1318−1325.

(13) D'Hahan, N.; Moreau, C.; Prost, A. L.; Jacquet, H.; Alekseev, A. E.; Terzic, A.; Vivaudou, M. Pharmacological Plasticity of Cardiac ATP-Sensitive Potassium Channels Toward Diazoxide Revealed by ADP. *Proc. Natl. Acad. Sci. U.S.A.* **1999**, *96*, 12162−12167.

(14) Topliss, J. G.; Sherlock, M. H.; Reimann, H.; Konzelman, L. M.; Shapiro, E. P.; Pettersen, B. W.; Schneider, H.; Sperber, N. Antihypertensive Agents. I. Non-Diuretic 2*H*-1,2,4-Benzothiadiazine 1,1-Dioxides. *J. Med. Chem.* **1963**, *6*, 122−127.

(15) Topliss, J. G.; Konzelman, L. M.; Shapiro, E. P.; Sperber, N.; Roth, F. E. Antihypertensive Agents. II. 3-Substituted 2*H*-1,2,4-Benzothiadiazine 1,1-Dioxides. *J. Med. Chem.* **1964**, *7*, 269−273.

(16) Parenti, C.; Costantino, L.; Di Bella, M. Heteroarylalkanoic Acids with Possible Antiinflammatory Activities. Part 8: The Scavenging of the Oxygen-Free Radicals. *Pharmazie* **1990**, *45*, 680−681.

(17) Petersen, H. J. Synthesis of 3-Amino- and 3-Substituted Amino-2*H*-1,2,4-Benzothiadiazine 1,1-Dioxides. *Acta. Chem. Scand.* **1973**, *27*, 2655−2660.

(18) de Tullio, P.; Pirotte, B.; Lebrun, P.; Fontaine, J.; Dupont, L.; Antoine, M. H.; Ouedraogo, R.; Khelili, S.; Maggetto, C.; Masereel, B.; Diouf, O.; Podona, T.; Delarge, J. 3-and 4-Substituted 4*H*-Pyrido[4,3-*e*]-1,2,4-Thiadiazine 1,1-Dioxides as Potassium Channel Openers: Synthesis, Pharmacological Evaluation, and Structure−Activity Relationships. *J. Med. Chem.* **1996**, *39*, 937−948.

(19) Pirotte, B.; de Tullio, P.; Lebrun, P.; Antoine, M. H.; Fontaine, J.; Masereel, B.; Schynts, M.; Dupont, L.; Herchuelz, A.; Delarge, J. 3-(Alkylamino)-4*H*-Pyrido[4,3-*e*]-1,2,4-Thiadiazine 1,1-Dioxides as Powerful Inhibitors of Insulin Release From Rat Pancreatic β-Cells: a New Class of Potassium Channel Openers? *J. Med. Chem.* **1993**, *36*, 3211−3213.

(20) Lebrun, P.; Arkhammar, P.; Antoine, M. H.; Nguyen, Q. A.; Hansen, J. B.; Pirotte, B. A Potent Diazoxide Analogue Activating ATP-Sensitive K^+ Channels and Inhibiting Insulin Release. *Diabetologia* **2000**, *43*, 723−732.

(21) Nielsen, F. E.; Bodvarsdottir, Th. B.; Worsaae, A.; MacKay, P.; Stidsen, C. E.; Boonen, H. C. M.; Pridal, L.; Arkhammar, P. O. G.; Wahl, Ph.; Ynddal, L.; Junager, F.; Dragsted, N.; Tagmose, T. M.; Mogensen, J. P.; Koch, A.; Treppendahl, S. P.; Hansen, J. B.; 6-Chloro-3-alkylamino-4*H*-thieno[3,2-*e*]-1,2,4-thiadiazine 1,1-Dioxide Derivatives Potently and Selectively Activate ATP Sensitive Potassium Channels of Pancreatic *β*-Cells. *J. Med. Chem.* **2002**, *45*, 4171−4187.

(22) Alemzadeh, R.; Fledelius, C.; Bodvarsdottir, T.; Sturis, J. Attenuation of Hyperinsulinemia by NN414, a SUR1/Kir6.2 Selective K^+-Adenosine Triphosphate Channel Opener, Improves Glucose Tolerance and Lipid Profile in Obese Zucker Rats. *Metabolism* **2004**, *53*, 441−447.

(23) Choi, J. K. NN-414. *Curr. Opin. Invest. Drugs* **2003**, *4*, 455−458.

(24) Böhm, H. J.; Schneider, G. Virtual Screening for Bioactive Molecules. In *Methods and Principles in Medicinal Chemistry*, Vol. 10; Mannhold, R., Kubinyi, H., Folkers, G., Eds.; Wiley−VCH: Weinheim, Germany, 2000.

(25) Stahura, F. L.; Bajorath, J. New Methodologies for Ligand-Based Virtual Screening. *Curr. Pharm. Des.* **2005**, *11*, 1189−1202.

(26) The SPECS database is available from http://www.specs.net.

(27) Irwin, J. J.; Shoichet, B. K. ZINC−A Free Database of Commercially Available Compounds for Virtual Screening. *J. Chem. Inf. Model.* **2005**, *45*, 177−182.

(28) http://zinc.docking.org.

(29) Mannhold, R.; Berellini, G; Carosati, E.; Benedetti, P. Use of MIF-based VolSurf Descriptors in Physicochemical and Pharmacokinetic studies. In *Molecular Interaction Fields in Drug Discovery*; Cruciani, G., Ed.; Methods and Principles in Medicinal Chemistry, Vol. 27; Wiley−VCH: Weinheim, Germany, 2005; pp 173−196.

(30) Pastor, M.; Cruciani, G.; McLay, I.; Pickett, S.; Clementi, S. GRid-INdependent Descriptors (GRIND): A Novel Class of Alignment-Independent Three-Dimensional Molecular Descriptors. *J. Med. Chem.* **2000**, *43*, 3233−3243.

(31) (a) Perruccio, F.; Mason, J.; Sciabola, S.; Baroni, M. FLAP: 4 Point Pharmacophore Fingerprints from GRID. In *Molecular Interaction Fields in Drug Discovery*; Cruciani, G., Ed.; Methods and Principles in Medicinal Chemistry, Vol. 27; Wiley−VCH: Weinheim, Germany, 2005; pp 83−102. (b) Baroni, M.; Cruciani, G.; Sciabola, S.; Perruccio, F.; Mason, J. S. A Common Reference Framework for Analyzing/Comparing Proteins and Ligands: FLAP Theory and Application. *J. Chem. Inf. Model.* **2007**, *47*, 279−294.

(32) Rishton, G. M. Reactive compounds and in vitro false positive in HTS. *Drug Discovery Today* **1997**, *2*, 382−384.

(33) Olah, M. M.; Bologa, C. G.; Oprea, T. I. Strategies for Compound Selection. *Curr. Drug Discovery Technol.* **2004**, *1*, 211−220.

(34) Nielsen, F. E.; Ebdrup, S.; Frost Jensen, A.; Ynddal, L.; Bodvarsdottir, T.; Stidsen, C.; Worsaae, A.; Boonen, H. C. M.; Arkhammar, P. O. G.; Fremming, T.; Wahl, P.; Kornø, H. T.; Hansen, J. B.; New 3-Alkylamino-4*H*-thieno-1,2,4-thiadiazine 1,1-Dioxide Derivatives Activate ATP Sensitive Potassium Channels of Pancreatic Beta Cells. *J. Med. Chem.* **2006**, *49*, 4127−4139.

(35) Arkhammar, P.; Wahl, P.; Gerlach, B.; Fremming, T.; Hansen, J. B. Establishment and Application of in Vitro Membrane Potential Assays in Cell Lines With Endogenous or Recombinant Expression of ATP-Sensitive Potassium Channels (Kir6.2/SUR1) Using a Fluorescent Probe Kit. *J. Biomol. Screen.* **2004**, *9*, 382−390.

(36) Schou, S. C.; Hansen, H. C.; Tagmose, T. M.; Boonen, H. C. M.; Worsaae, A.; Drabowski, M.; Wahl, P.; Arkhammer, P. O. G.; Bodvarsdottir, T.; Antoine, M. H.; Lebrun, P.; Hansen, J. B. Synthesis and Pharmacological Evaluation of 4*H*-1,4-Benzothiazine-2-Carbonitrile 1,1-Dioxide and *N*-(2- Cyanomethylsulfonylphenyl)Acylamide Derivatives As Potential Activators of ATP Sensitive Potassium Channels. *Bioorg. Med. Chem.* **2005**, *13*, 141−155.

(37) The VolSurf program, version 4.1, is distributed by Molecular Discovery Ltd., http://www.moldiscovery.com.

(38) (a) Crivori, P.; Cruciani, G.; Carrupt, P. A.; Testa, B. Predicting Blood−Brain Barrier Permeation from Three-Dimensional Molecular Structure. *J. Med. Chem.* **2000**, *43*, 2204−2216. (b) Cruciani, G.; Meniconi, M.; Carosati, E.; Zamora, I.; Mannhold, R. VolSurf: a Tool for Drug ADME Properties Prediction. In *Drug Bioavailability. Estimation of Solubility, Permeability, Absorption and Bioavailability*; Van de Waterbeemd, H., Lennernaes, H., Artursson, P., Eds.; Wiley−VCH: Weinheim, Germany, 2003; pp 406−419. (c) Oprea, T. I.; Matter, H. Integrating Virtual Screening in Lead Discovery. *Curr. Opin. Chem. Biol.* **2004**, *8*, 349−358.

(39) de Tullio, P.; Boverie, S.; Becker, B.; Antoine, M. H.; Nguyen, Q. A.; Francotte, P.; Counerotte, S.; Sebille, S.; Pirotte, B.; Lebrun, P. 3-Alkylamino-4*H*-1,2,4-benzothiadiazine 1,1-Dioxides as ATP-Sensitive Potassium Channel Openers: Effect of 6,7-Disubstitution on Potency and Tissue Selectivity. *J. Med. Chem.* **2005**, *48*, 4990−5000.

(40) Sheridan, R. P.; Rusinko, A., 3rd; Nilakantan, R.; Venkataraghavan, R. Free in PMC Searching for Pharmacophores in Large Coordinate Data Bases and Its Use in Drug Design. *Proc. Natl. Acad. Sci. U.S.A.* **1989**, *86*, 8165−9.

(41) The Almond program, version 3.3, is distributed by Molecular Discovery Ltd., http://www.moldiscovery.com.

(42) Fontaine, F.; Pastor, M.; Sanz, F. Incorporating Molecular Shape into the Alignment-free GRid-INdependent Descriptors (GRIND). *J. Med. Chem.* **2004**, *47*, 2805−2815.

(43) Gregori-Puigjané, E.; Mestres, J. SHED: Shannon Entropy Descriptors from Topological Feature Distributions. *J. Chem. Inf. Model.* **2006**, *49*, 1615−1622.

(44) Carosati, E.; Cruciani, G.; Chiarini, A.; Budriesi, R.; Ioan, P.; Spisani, R.; Spinelli, D.; Cosimelli, B.; Fusi, F.; Frosini, M.; Matucci, R.; Gasparrini, F.; Ciogli, A.; Stephens, P. J.; Devlin, F. J. Calcium Channel Antagonists Discovered by a Multidisciplinary Approach. *J. Med. Chem.* **2006**, *49*, 5206−5216.

(45) Dabrowski, M.; Wahl, P.; Holmes, W. E.; Ashcroft, F. M. Effect of Repaglinide on Cloned Beta Cell, Cardiac and Smooth Muscle Types of ATP-Sensitive Potassium Channels. *Diabetologia* **2001**, *44*, 747−756.

(46) Arnaud Merglen, A.; Theander, S.; Rubi, B.; Chaffard, G.; Wollheim, C. B. Maechler, P. Glucose Sensitivity and Metabolism-Secretion Coupling Studied during Two-Year Continuous Culture in INS-1E Insulinoma Cells. *Endocrinology* **2004**, *145*, 667−678.

(47) (a) Goodford, P. J. A Computational Procedure for Determining Energetically Favorable Binding Sites on Biologically Important Macromolecules. *J. Med. Chem.* **1985**, *28*, 849−857. (b) Carosati, E.; Sciabola, S.; Cruciani, G. Hydrogen Bonding Interactions of Covalently Bonded Fluorine Atoms: From Crystallographic Data to a New Angular Function in the GRID Force Field. *J. Med. Chem.* **2004**, *47*, 5114−5125.

(48) The GRID package, version 22, is distributed by Molecular Discovery Ltd., http://www.moldiscovery.com.

(49) Baroni, M.; Costantino, G.; Cruciani, G.; Riganelli, D.; Valigi, R.; Clementi, S. Generating Optimal Linear PLS Estimations (GOLPE): An Advanced Chemometric Tool for Handling 3D-QSAR Problems. *Quant. Struct. Act. Relat.* **1993**, *12*, 9−20.

(50) The Golpe program, version 4.5.12, is distributed by MIA srl., http://www.miasrl.com.

JM061440P